J Mater Sci (2007) 42:149–155
DOI 10.1007/s10853-006-1087-3

Study of the dc resistivity and thermoelectric power in Mn-substituted Ni–Zn ferrites

A. A. Sattar · H. M. El-Sayed · K. M. El-Shokrofy · M. M. El-Tabey

Received: 4 May 2005 / Accepted: 4 January 2006 / Published online: 14 November 2006

Abstract The electrical resistivity and thermoelectric power as a function of temperature and Mn concentration for $Ni_{0.6-t}\,Mn_t\,Zn_{0.4}Fe_2O_4$ (t = 0, 0.1, 0.2, 0.3, 0.4 and 0.5) have been studied. It was observed that temperature variation of resistivity exhibits two breaks. Each break is associated with a change in activation energy. The activation energy in the paramagnetic region is found to be greater than that in the ferrimagnetic one. Moreover, it was found that the resistivity increases with increasing Mn content. The sign of thermoelectric power measurements revealed n-type conduction for all investigated samples. The results are explained according to the spin polaron model.

Introduction

Amongst all ferrites, Ni–Zn ferrites are the most versatile because of their technological applications. These ferrites have high resistivity (i.e. low eddy current losses), relatively low permeability and low saturation magnetization. On the other hand, Mn–Zn ferrites have high initial permeability and low resistivity (100Ω cm) [1]. The magnetic applications require in addition to high resistivity, high permeability as well as high saturation magnetization. Therefore, many authors [2–7] studied the combination of these two ferrites in order to obtain ferrites with favorable magnetic and electric properties especially at high frequencies. Amarendra et al. [2, 3] studied the microstructure, magnetic properties and the dc resistivity of $Mn_xNi_{0.5-x}Zn_{0.5}Fe_2O_4$ ferrites prepared by citrate precursor method. The samples were sintered at different temperatures in air atmosphere. They found that, for all sintering temperatures, the saturation magnetization, firstly, increased and then decreased continuously with increasing Mn-concentration. However, the resistivity decreased (about two order of magnitude) with increasing Mn-content. In our previous work, the magnetic properties of Mn substituted Ni–Zn ferrites were improved when the samples were prepared by standard ceramic technique and were finally sintered in nitrogen atmosphere [8]. The present work is devoted to study the electrical resistivity and thermoelectric power for the same samples of $Ni_{0.6-t}\,Mn_tZn_{0.4}Fe_2O_4$ ferrites.

Experimental procedure

Ferrite samples with chemical formula $Ni_{0.6-t}\,Mn_t\,Zn_{0.4}Fe_2O_4$ (t = 0, 0.1, 0.2, 0.3, 0.4, 0.5,) were prepared by conventional ceramic method. High purity, 99.99%, of NiO, ZnO, Fe_2O_3 and $MnCO_3$ were mixed together according to their molecular weights. The mixture of each composition was ground to a very fine powder and presintered at 900°C for 15 h. The presintered mixture was ground again and pressed under a pressure of 3.8×10^8 Pa into tablet form. The samples were

A. A. Sattar (✉) · H. M. El-Sayed
Physics Department, Faculty of Science, Ain Shams University, Cairo, Egypt
e-mail: Adel_sattar@maktoob.com

K. M. El-Shokrofy · M. M. El-Tabey
Basic Engineering Science Department, Faculty of Engineering, Minufia University, Shebin El-Kom, Egypt

finally sintered at 1300°C for 4 h in two cycles and then slowly cooled in N_2 atmosphere to room temperature. X-ray diffraction patterns were performed using a diffractometer (type X'Pert Graphics & Identify) with Cu Kα radiation.

The dc resistivity of the samples was measured using the two-probe method where In–Hg is used as a contact material. For measuring thermo-e.m.f. the sample is firmly fixed between two copper electrodes. An auxiliary heater is fixed to the lower electrode in order to maintain a temperature gradient of about 12°C/cm for all investigated samples. The sign of thermo e.m.f was taken as that of the upper electrode. The temperature was measured using a chromel – alumel thermocouple. The accuracy in resistivity and thermoelectric power measurements are 1% and 2% respectively.

Results and discussion

X-ray measurements

The X-ray diffraction patterns showed that all investigated samples are formed in cubic single spinel phase. The interplanar spacing is calculated according to Bragg's law and hence the average lattice parameter (a) is obtained. The theoretical lattice parameter is calculated using the equation [9]

$$a_{th} = (8/3\sqrt{3})[(r_A + R_O) + \sqrt{3}(r_B + R_O)]$$

where R_O is the radius of the oxygen ion (1.32Å), r_A and r_B are the ionic radii of tetrahedral and octahedral sites, respectively. To calculate r_A and r_B, the following cation distribution is assumed

$$(Zn_{0.4}\ Mn_{0.8t}\ Fe_{0.6-0.8t})\ [Mn_{0.2t}\ Ni_{0.6-t}Fe_{1.4+0.8t}]\ O_4 \quad (1)$$

Such cation distribution is based on the fact that, 80% of Mn-ions occupy the tetrahedral position (A-site) and the remaining, 20%; occupy the octahedral position (B-site) [10]. Moreover, Zn ions prefer to occupy the tetrahedral sites while Ni ions occupy the octahedral sites. The ionic radius for each site is calculated according to the following equations [9]

$$r_A = [0.4r_{Zn2+} + 0.8tr_{Mn2+} + (0.6 - 0.8t)r_{Fe3+}]$$

$$r_B = [0.2tr_{Mn2+} + (0.6 - t)r_{Ni2+} + (1.4 + 0.8t)r_{Fe3+}]/2$$

where r^{2+}_{Zn}, r^{2+}_{Mn}, r^{3+}_{Fe} and r^{2+}_{Ni} are the ionic radii of zinc, manganese, iron and nickel respectively. The values of the ionic radii are taken from ref. [11] where the ionic radius depends on its coordination number. Figure 1 shows the variation of the experimental and theoretical lattice parameter with Mn-concentration for all samples. Firstly, it is clear that the lattice parameter increases linearly with Mn-concentration. Such a behavior could be attributed to the replacement of the Ni^{2+} ion which has a small radius (0.72Å) by the Mn^{2+} ion which has a larger radius (0.8Å). Secondly, it is also noticed that the experimental values of the lattice parameter a_{exp} are greater than those of the theoretical ones a_{th}. This may be attributed to the formation of Fe^{2+} ions, during the sintering process, which have a larger ionic radius than those of Fe^{3+} ions. It is obvious that the difference between a_{th}. and a_{exp} decreases with increasing Mn-concentration. This led us to conclude that the amount of Fe^{2+} ions decreases with increasing Mn-concentration. Finally, it is valuable to note that the lattice parameter of the unsubstituted sample, $t = 0$, is (8.373Å) which is in agreement with those previously reported (8.384Å, and 8.381Å) [12, 13].

Electrical resistivity

The temperature dependence of the electrical resistivity (represented as log ρ versus 10^3/T) for the sample with $t = 0.4$ is shown in Fig. 2. Such a curve represents an example for the other samples. It is clear that the electrical resistivity has a semiconducting behavior which could be described as

$$\rho = \rho_o \exp -(E/KT)$$

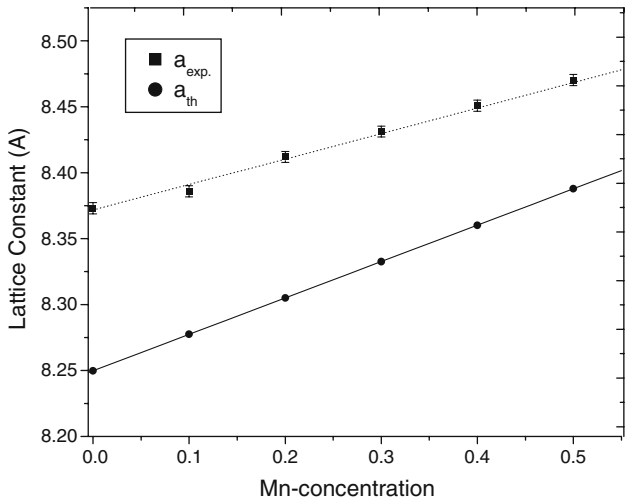

Fig. 1 Changes of the lattice parameter a (Å) with Mn-concentration (t)

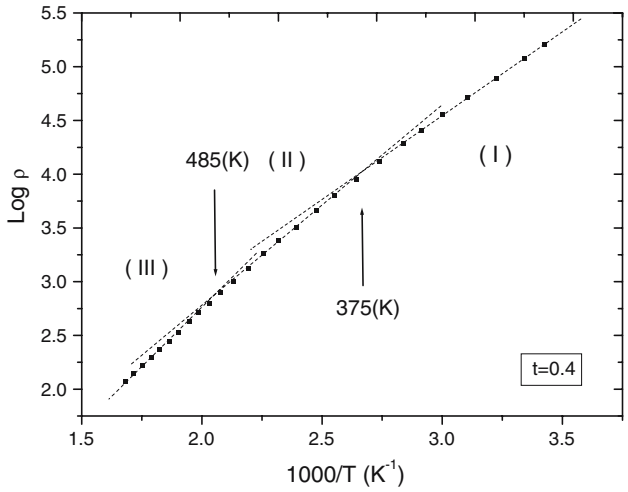

Fig. 2 Variation of resistivity with temperature for sample with $t = 0.4$

where E is the activation energy, K is Boltzmann constant and ρ_o is a temperature independent constant.

The variation of resistivity with temperature, for all samples, could be divided into three regions. The first one extends from room temperature up to about 380 K where a kink is observed. This region is almost independent of Mn concentration. The conduction phenomenon in this region is attributed to impurities [14–16]. Another kink is observed. However, the temperatures at which the kink occurs depend on Mn content. By comparing the values of the temperatures at this kink, $(T_c)_{elect}$ with Curie temperatures, $(T_c)_{mag.}$ determined from magnetic measurements (Table 1), one can attribute this kink to the magnetic transition from ferri- to paramagnetic state.

Table 1 shows also that the activation energies of the ferrimagnetic (E_{ferri}) and paramagnetic regions (E_{para}) increase with increasing Mn-concentration. Such an increase in activation energy could be attributed to the increase of lattice parameter with Mn- concentration. Moreover, the values of activation energies E_{ferri} are greater than the transition energy between Fe^{2+} and Fe^{3+} (0.2 eV) [13]. It was reported that [15], if E_ρ is higher than 0.2 eV then the conduction mechanism is predominantly due to small polaron than the electron hopping mechanism. Thus, our results support the small polaron hopping mechanism.

Figure 3 shows the variation of electrical resistivity ρ with Mn-concentration, at room temperature. It is clear that the electrical resistivity increases with increasing Mn content. This behavior could be interpreted in terms of the content of Fe^{2+} ions, which results during the sintering process due to the oxygen loss and Zn volatilization [3]. The concentration of Fe^{2+} ions in each sample is estimated from the difference between the experimental and theoretical values of the lattice parameters and is represented also in Fig. 3. It is clear that the concentration of Fe^{2+}-ions decreases with increasing Mn content which is in agreement with the fact that manganese makes a suppression to the ferrous (Fe^{2+}) ion formation [17]. The decrease of Fe^{2+} ion concentration leads the resistivity to increase as the conduction is due to electron hopping between Fe^{2+} and Fe^{3+} ions.

Figure 4 shows the changes of (E_{ferri}) and (E_{para}) with Mn concentration. It is obvious that (E_{para}) is greater than (E_{ferri}) and the difference between them increases with Mn concentration. The increase of the activation energy from order to disorder state was attributed to the volume expansion at T_c [18]. Such

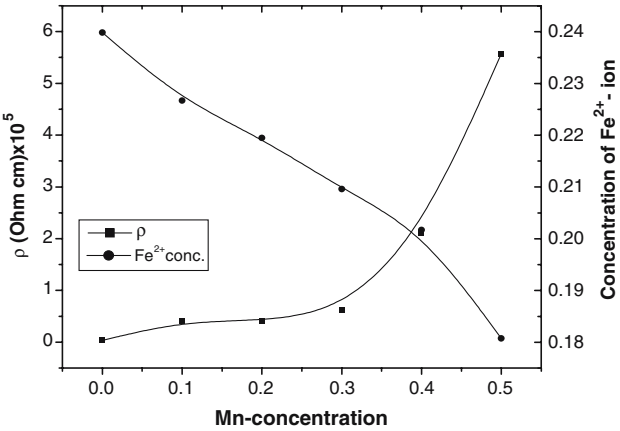

Fig. 3 Variation of resistivity(ρ) and the concentration of Fe^{2+}-ion with Mn-concentration (t)

Table 1 Variation of activation energies and Curie temperatures with Mn-concentration

Mn-conc. (t)	E_{ferri} (eV) second region	E_{para} (eV) thrid region	E_μ (eV) second region	$(T_C)_{elect.}$ (K)	$(T_C)_{mag.}$ (K)
0	0.711	0.737	0.704	649	657
0.1	0.769	0.811	0.767	610	619
0.2	0.777	0.83	0.769	588	579
0.3	0.82	0.881	0.82	540	538
0.4	0.848	0.945	0.845	485	483
0.5	0.871	0.994	0.865	380	378

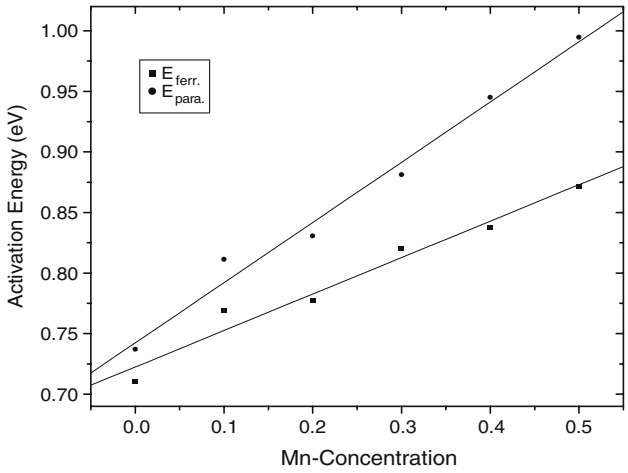

Fig. 4 Changes of activation energies with Mn-concentration

expansion is known to be accompanied by an endothermic peak in differential scanning calorimetry (DSC). However, the DSC of our samples, Fig. 5, indicated good thermal stability from room temperature up to temperatures higher than T_c. Therefore, the explanation of the increase of the activation energy in terms of the volume expansion is not the suitable one. The change in activation energy may also be accounted for using the spin polaron model. According to this model, the total energy of the spin polaron is given by [19]

$$E_S = \frac{5\hbar^2\pi^2}{6m}\left(\frac{4mJ_2}{\hbar^2\pi a^3}\right)^{2/5} - J_1 \qquad (2)$$

where m is the electron mass, a is the lattice parameter, J_1 is the exchange energy between the spin of the conduction electron and ion spins and J_2 is the exchange energy between the ion spins. The condition for spin polaron formation is that $J_1 > J_2$ which means that the moments are fully oriented parallel to that of the conduction electrons. For $T < T_c$, the ionic magnetic moments are parallel (i.e. $J_2 > J_1$) and the magnetic spin polaron has a small effect. On the other hand, for $T > T_c$, the magnetic ionic moments are randomly oriented (i.e. $J_2 < J_1$), so the contribution of magnetic spin polaron becomes effective. Therefore, the effective mass of the conduction electrons will increase due to the magnetic polarization of the spin polaron [20, 21]. This means that, the activation energy of spin polaron (E_s) should be added to that in the ferrimagnetic region i.e.

$$E_{(\text{para})} = E_{(\text{Ferri})} + E_s \qquad (3)$$

Thus the activation energy in the paramagnetic region $E_{(\text{para})}$ must always be greater than that in the ferrimagnetic one, $E_{(\text{ferri})}$. Furthermore, according to Methafessel et al. [22], the activation energy E_s is roughly proportional to the paramagnetic susceptibility (χ_{para}) since it depends on the extent to which the lattice spins can swing parallel to the spins of the conduction electrons. Moreover, according to the assumed cation distribution, the paramagnetic susceptibility (χ_{para}) of the investigated samples is expected to increase with Mn concentration. Hence E_s is expected to increase with increasing Mn concentration. This explains the increase of the difference between $E_{(\text{para})}$ and $E_{(\text{ferri})}$ with increasing Mn-concentration, Fig. 4.

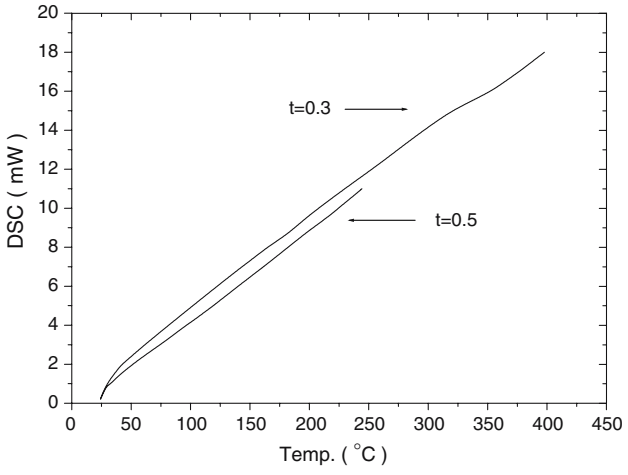

Fig. 5 The temperature dependence of DSC for samples with $t = 0.3$ and $t = 0.5$

Thermoelectric power

Figure 6 shows the temperature dependence of thermoelectric power, represented as (α/198). It is obvious that the sign of α is negative, for all investigated samples, which indicates that the dominant charge carriers are electrons, i. e the samples are n-type semiconductor. The variation of (α/198) with temperature could also be divided into three distinct regions as in case of resistivity curves. The transition temperature of each region is nearly close to that obtained from the resistivity measurements. This is clarified by plotting both resistivity and thermoelectric power on the same graph, Fig. 7, for the sample with $t = 0.4$ as an example.

The change of α with temperature in the first region indicates a change in the number of charge carriers that set up from the impurity levels. Such a result supports the discussion of the resistivity in the same

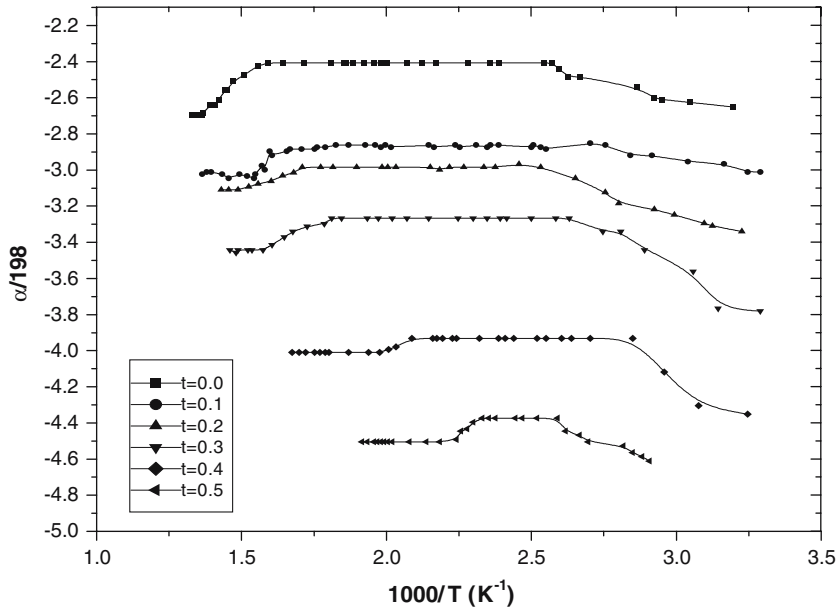

Fig. 6 The temperature dependence of thermo-power of the investigated samples

region. The most striking feature is that in the second region, although the resistivity decreases in this region, the value of α is almost independent of temperature which characterizes the hopping mechanism and supports our previous results. The Curie temperatures are also determined by plotting the relation between (dα/d(1/T)) against (1/T) around T_c, Fig. 8. The onset of the curve determines T_C. It is obvious that during the magnetic transition there is a rapid change in (dα/d(1/T)) with temperature which indicates that the thermoelectric power is a sensitive parameter for the magnetic transition. From the temperature dependence of α, one can observe also that the absolute value of thermoelectric power in the third region (after Curie temperature) is greater than that in the second one. This could be interpreted in terms of spin polaron formation, where after T_C the moving electron will tend to polarize the ion spins near it, in ferromagnetic sense. Hence, if the band is sufficiently narrow the electron will be trapped in the ferromagnetic spin cluster [23]. Therefore, the number of electrons which share in conduction reduces and hence, according to [24], the absolute value of thermoelectric power increases.

To get more confirmation about the conduction mechanism, the charge carrier mobility (μ) is calculated according to the known formula [25]

$$\mu = (1/ne\rho)$$

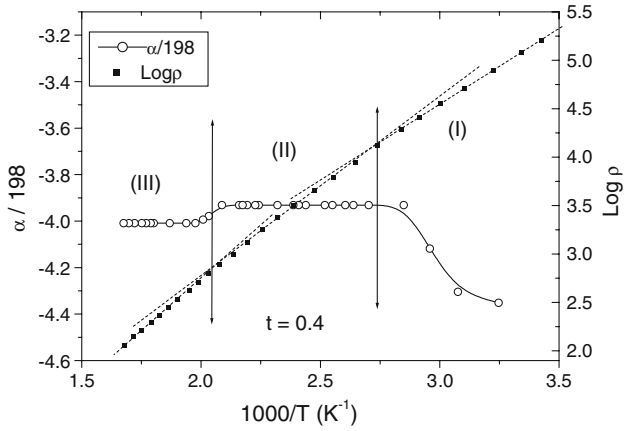

Fig. 7 Variation of resistivity and thermoelectric power with temperature for sample with t = 0.4

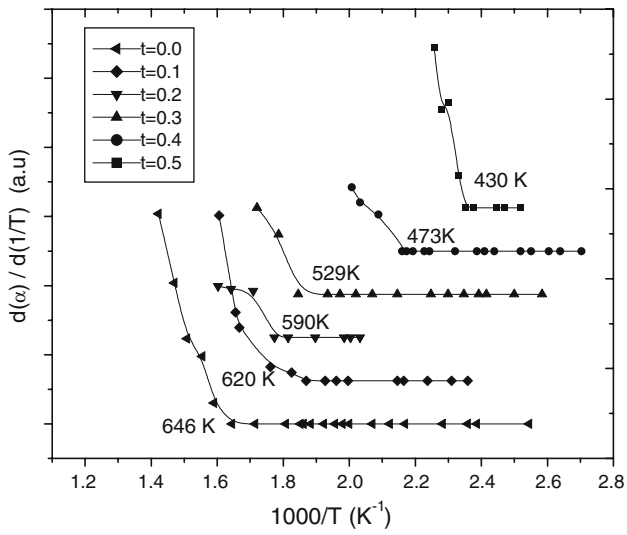

Fig. 8 The temperature dependence of (dα/d (1/T)) for different Mn-concentration

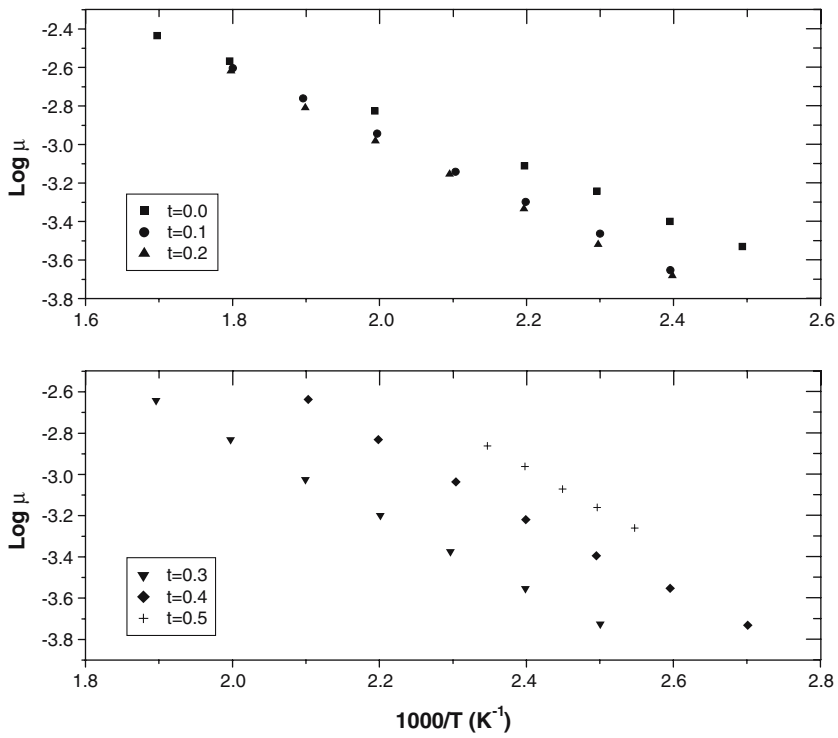

Fig. 9 The dependence of mobility (logμ) on temperature (1000/T) for different Mn-concentration

where n is the charge carrier concentration and e is the electronic charge. The value of n is calculated from the relation

$$n = N_o \exp(-e\alpha/K)$$

where N_o is the density of states which represents the Fe^{3+}-ion concentration. Figure 9 shows the temperature dependence of the mobility in the second region. It is clear that the mobility increases strongly with increasing temperature which gives further evidence for the hopping mechanism. The calculated activation energy of the mobility E_μ is reported in Table 1. It is seen that the values of E_μ are very close to those of E_{ferri} . This means that the energy is consumed mainly in moving the polaron and not for further generation of charge carriers.

Conclusions

(1) On Mn ion substitution both the lattice parameter and the resistivity of Ni–Zn ferrites increase.
(2) The activation energies of conduction in both order and disorder states increase with increasing the Mn-concentration
(3) The Curie temperature, T_C, shifts to lower values as the Mn content increases.
(4) The negative sign of the thermoelectric power indicates that the majority of charge carriers are electrons.
(5) The results support the polaron hopping conduction mechanism.

References

1. Chikazumi S, Charap S (1964) Physics of Magnetism. John Wiley and Sons, Inc., New York, London, Sydney
2. Singh AK, Goel TC, Mendiratta RG (2002) J Appl Phys 92(7):3872
3. Singh AK, Verma A, Thakur OP, Prakash C, Goel TC, Mendiratta RG (2002) Jpn J Appl Phys, 41, 5142
4. Bera J, Samanta AK, Aravind M (2000) Procc. Of (ICF 8), Kyoto and Tokyo, Japan, 536
5. Singh AK, Goel TC, Mendiratta RG (2004) Phys Stat Sol (a) 201:1453
6. Singh AK, Goel TC, Mendiratta RG (2003) Jpn J Appl Phys 42:2690
7. Rezlescu E, Sachelarie L, Popa PD, Rezlescu N (2000) IEEE Trans Magn 36(6):3962
8. Sattar AA, El-Sayed HM, El-Shokrofy KM, El-Tabey MM (2005) J Mater Eng Perform 14(1):99
9. Mazen SA, Abdallah MH, Sabrah BA, Hashem HAM (1992) Phys Stat Sol(a) 134, 263
10. Petil F, Lenglet M (1993) Solid State Commun 86:67
11. Shannon RD and Prewitt CT (1970) Acta Crystal B26:1046
12. Globus A, Pascaer H, Cagan V (1977) J Physique Colloque C1, supple‘ment au n° 4 38:C1

13. Rezlescu N, Rezlescu E, Pasnicu C, Craus ML (1994) J Phys I Condens Matter 6:5707
14. Patil MG, Mahajan VC, Lotke SD, Bhise BV, Patil SA (1994) Solid State Commun 91(8):667
15. Patil BL, Sawant SR, Patil SA, Patil Rn (1994) J Mater Sci 29:175
16. Bhise BV, Lotke SD, Patil SA (1996) Phys Stat Sol(a) 157:411
17. Smit J, Wijn PJ (1959) Ferrites, Johnwiley and Sons, p 233
18. Satar AA, Wafik AH, El-Sayed HM (2000) Procedings of (ICF 8), Koyoto and Tokyo, Japan
19. Mott NF, Davis EA (1971) Electronic processes in non-crystalline materials. Clarendon press, Oxford, p 175
20. Wolfram T, Callaway HJ (1962) Phys Rev 127:1605
21. Zilichikhis AL, Irkhin YP (1969) Sov Phys Solid State 10:1554
22. Methafessel S, Mattis DC (1968) Hand Buch der Physik 127:439
23. Austin IG, Mott NF (1969) Adv Phys 18:41
24. Jain GC, Berry WB (1972) Transport properties of solids and solid state energy conversion, Tata McGraw-Hill , C-98 South Extension II, New Delhi, p 37
25. Reddy PV, Reddy VD, Ravinder D (1991) Phys Stat Sol(a) 127, 439